Progress In Electromagnetics Research C, Vol. 133, 81–95, 2023

Improving Mutual Coupling in MIMO Antennas Using Different Techniques

Mostafa A. Nassar[1, *], Heba Y. Soliman[1], Rania M. Abdallah[1], and Esmat A. F. Abdallah[2]

Abstract—Two different MIMO antennas configurations are proposed in this paper for operation around 30 GHz with a bandwidth of 0.8 GHz. The proposed configurations are applicable in 5G, 6G, and radar systems in Ka-band systems. Each of the proposed configurations consists of four identical rectangular elements where each element is connected to an impedance transformer for impedance mismatch improvement. Due to the close existence of antenna elements, mutual coupling can seriously degrade the gain, signal to noise ratio, matching characteristics, and efficiency of the MIMO antenna systems. To overcome performance degradation, several techniques such as Curved Edges (CE), Defected Ground Structure (DGS), and Band Gap Structure (BGS) are implemented. Simulation was carried out using the commercial Computer Simulation Technology (CST) and High Frequency Structure Simulation Software (HFSS). Prototypes are fabricated and measured. The experimental results show good agreement with the simulated ones. Improvement in the mutual coupling value from −21.4 dB to −27.2 dB also proves the practicality of this design.

1. INTRODUCTION

The exponential growth of wireless devices over time has made it possible to present more complex standards for communication networks [1, 2]. In order to meet the demands for high-throughput, high data rates, and additionally provide high-speed connectivity on the user end, 4G LTE has successfully incorporated a number of commercial services inside a currently deployed network [3, 4]. However, this huge improvement has raised troubles associated with bandwidth scarcity, which in addition restricts the required advancements, at the same time as consuming restricted spectrum up to 2.5 GHz [5, 6]. Available spectrum on the millimeter-waves (MMWs) is anticipated to perform the destiny 5G needs of excessive capacity and throughput. Signal fading, path loss attenuations, and atmospheric absorptions are essential obstacles that must be resolved on the MMW spectrum [7, 8]. Additionally, a thorough and radical RF link analysis is required to account for the channel parameters within the radio wave propagation medium [9]. Multiple-input multiple-output (MIMO) structures have received interest in current studies because of its functionality to operate multi-antennas simultaneously, which additionally affects in growth of channel capability with no extra spectrum or transmitted energy requirements [10]. MIMO architectures permit the availability of practical and dependable communications with the benefits of better data rates and multi-Gbps throughput.

Designing a new antenna for 5G applications is more demanding at MMW frequencies wherein flexibility of architecture, efficiency, reliability, and compatibility with MIMO structures are primary concerns to attain excessive spectral efficiency, in addition to decrease multipath fading [11, 12]. The 5G MIMO antenna's general requirements include having enough bandwidth to support the simultaneous

Received 31 March 2023, Accepted 15 May 2023, Scheduled 27 May 2023
* Corresponding author: Mostafa A. Nassar (m.assem@eng.psu.edu.eg).
[1] Electrical Engineering Department, Port Said University, Port Said, Egypt. [2] Microstrip Department, Electronics Research Institute, Cairo, Egypt.

operation of many services, enough gain to deal with atmospheric attenuations and absorptions, and being simple to incorporate into MIMO systems [13]. Additionally, any device that uses the considered antenna geometry must be compact [14].

To reduce the performance impact of adjacent antennas, MIMO antenna designs demand for minimizing mutual coupling and enhancing isolation among narrow-spaced antenna elements [15], which is challenging to do given the limited space allotted for antenna placement in devices. There have been several attempts to reduce the mutual coupling between MIMO antenna parts [16, 17]. The advantage of MMW frequencies is smaller antenna size, which enables matching of a few parts in a constrained space with less mutual coupling.

Due to their flat, small, and resilient shape, patch antennas have attracted significant interest from manufacturers of wireless devices and integrated circuits [18]. Small directivity and limited bandwidth are the main challenges; however they can both be greatly overcome by employing a variety of approaches. Another issue with patch antennas is their excessive isolation, which is particularly problematic for broadband range [19]. Diverse tactics, such as defected ground structures, decoupling networks, electromagnetic band-gap structures, array-antenna decoupling surfaces, neutralization lines,and parasitic elements, have been used in such situations to suppress mutual coupling among MIMO antenna elements. Wideband antenna isolation, however, requires multiple mechanisms and tactics to improve isolation in particular frequency bands [20]. Defected ground structure (DGS), for instance, is a technique that was developed to improve antenna performance by taking use of flaws in the ground's planar geometry [21]. These flaws are to blame for the disturbances that disrupt both the continuity of surface currents and the homogeneity of the ground plane. When being appropriately aligned to enable effective coupling with the feed line, DGS is a symmetrical system functioning as resonant gaps that may be delivered instantly beneath or on both sides of a microstrip line. DGS also modifies the ground's protection of the current distribution based on its shape and length.

Because of their matchless electromagnetic properties, Band Gap Structures (BGSs) have recently received a lot of interest. Periodic structures like metal patches and dielectric bars are commonly used to realize BGS. They have distinct band gap characteristics for electromagnetic waves, which result in a variety of applications such as low profile and good performance microstrip antennas [22].

The primary goal of this research is to develop and optimize the performance of two MIMO antennas for millimeter-wave applications, with a focus on improving mutual coupling. This research utilizes a combination of different techniques to achieve this goal, including advanced antenna design, simulation, and prototype fabrication. The proposed MIMO antennas are designed to operate around 30 GHz, which is a promising frequency for future wireless communication networks. The design and optimization process is carried out using the CST Microwave studio and High-Frequency Structure Simulator (HFSS) software, which allow for precise modeling and analysis of the antenna's performance. The optimization process involves adding mutual coupling reduction techniques between the antennas such as DGS and BGS to reduce the mutual coupling effect, while maintaining good impedance matching and radiation pattern. Finally, a prototype of the proposed MIMO antennas is fabricated, and the measured results are compared with the simulated ones to validate the design. The results of this research contribute to the development of efficient and reliable MIMO systems for future wireless communication networks, where high-speed data transfer and low latency are essential.

The rest of this paper is organized as follows. In Section 2, a detailed design of a single element and the antenna parameters which will be used to make the MIMO antenna operating at 30 GHz are presented. Section 3 presents the design of a MIMO antenna consisting of two antenna elements, and detailed values of the parameters of the MIMO antenna, as well as introduction of three techniques to reduce the values of the mutual coupling between the antenna elements, are given. In Section 4, we transfer the techniques used to reduce the mutual coupling mentioned in Section 3 into a four MIMO antenna. Section 5 draws the conclusion.

2. DESIGN OF A SINGLE ANTENNA AT 30 GHZ

The antenna is designed to operate at a frequency of 30 GHz and bandwidth of around 0.8 GHz, which means that the fractional bandwidth is about 2.6%. As the fifth generation 5G applications require more than 0.2 GHz bandwidth [23], this antenna is considered suitable for 5G applications [24]. The

proposed antenna was designed using CST Microwave Studio software and HFSS. The design was built on a substrate of Rogers RT5880 ($\varepsilon_r = 2.2$, $h = 0.25$ mm, $\tan\delta = 0.001$), and the conductor is copper (annealed) for patches, microstrip lines, impedance transformers, and ground plane.

The single antenna element connected to a microstrip feed line of width 0.75 mm to get 50 Ω is shown in Figure 1 where the dimensions of the patch are $Lp \times Lp$ mm. Also, a quarter wavelength impedance transformer of width 0.05 mm and length Li of 1 mm is positioned between the patch and the microstrip feed line to enhance the impedance matching. All the dimensions were calculated using

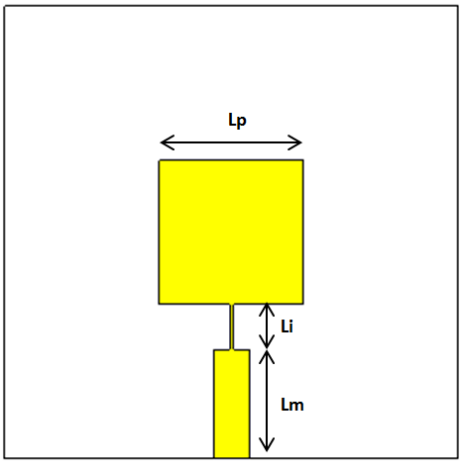

Figure 1. Single patch antenna design.

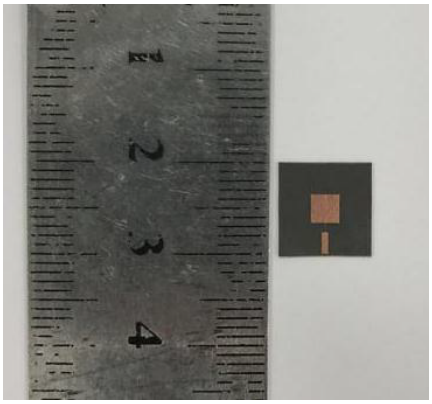

Figure 2. Photo of fabricated single patch antenna.

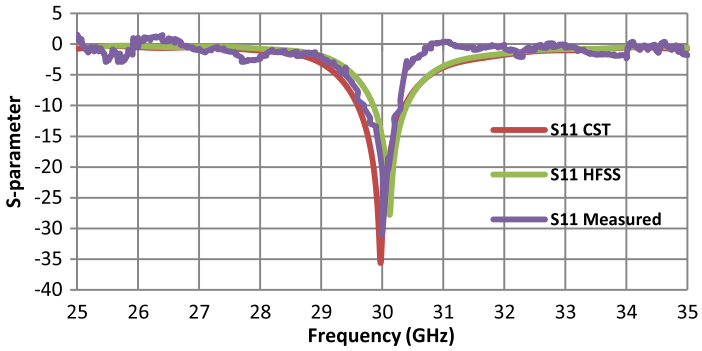

Figure 3. S_{11} of the single patch antenna.

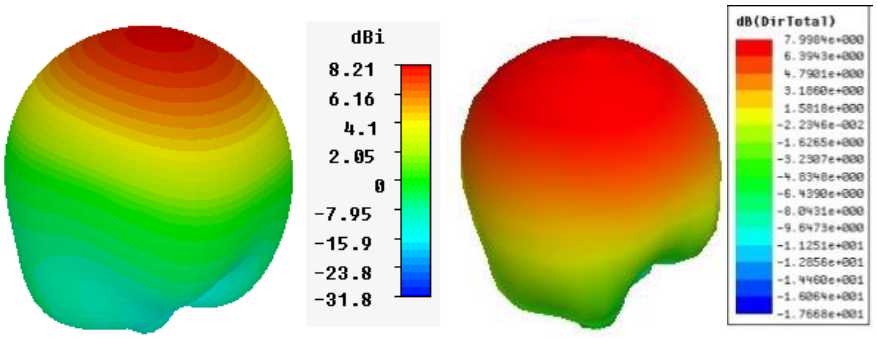

(a) (b)

Figure 4. 3D radiation pattern of a single element at 30 GHz, (a) CST, (b) HFSS.

antenna equations and more than one microstrip calculator according to the frequency band. All the fabrication and measurement were done in the Electronics Research Institute (ERI) in Cairo, Egypt. Figure 2 shows a photograph for the fabricated single patch antenna. Table 1 shows all the detailed dimensional parameters. The S-parameter S_{11} for this antenna is shown in Figure 3, and it displays an excellent matching of -35 dB at 30 GHz. Figure 4 demonstrates that the 3D radiation pattern has a symmetrical shape and that the directivity calculated using CST and HFSS is approximately 8 dBi. Figure 5 shows the maximum gain over frequency showing a gain of around 7.5 dBi at 30 GHz. From Figure 6, the real part of input impedance is found to be 50 ohms, and the imaginary part is around zero, which means perfect matching.

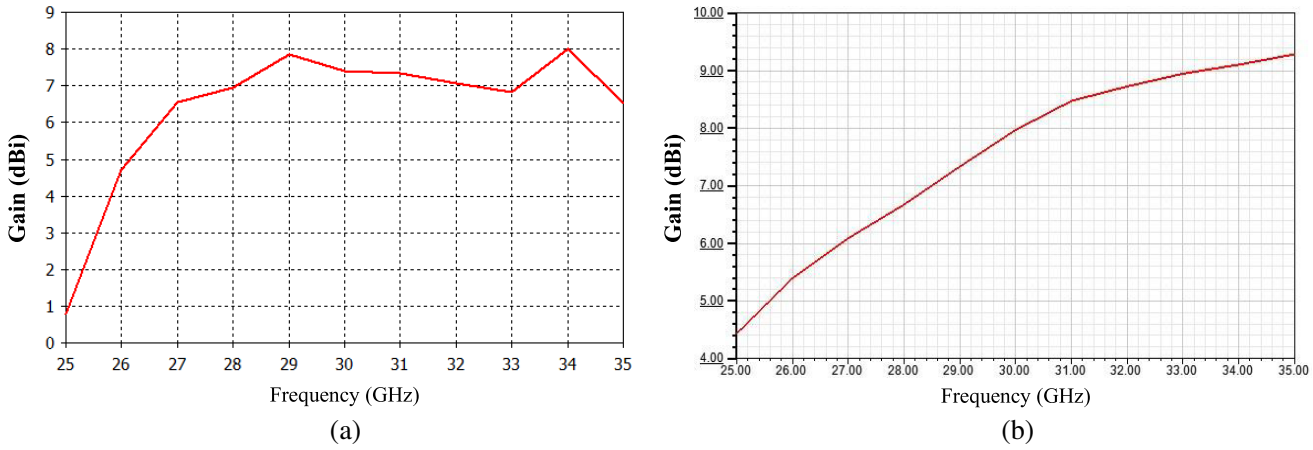

Figure 5. Maximum gain against frequency, (a) CST, (b) HFSS.

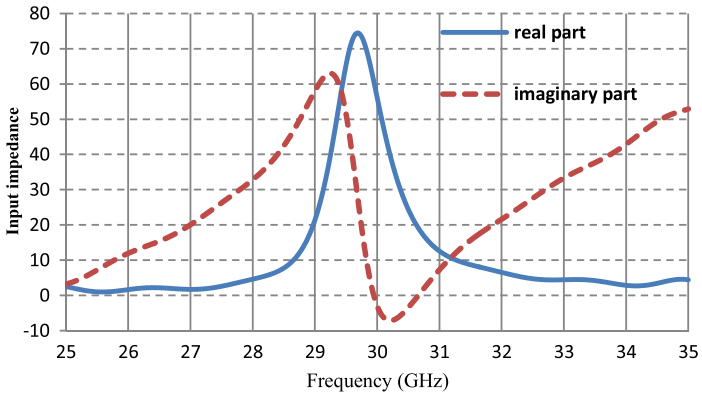

Figure 6. Real and imaginary part of input impedance against frequency.

3. DESIGN OF A SINGLE BAND TWO ELEMENTS MIMO ANTENNA

In this section, we introduce how MIMO configuration could operate using the antenna presented in the previous section as a single element, and we discuss some techniques to reduce mutual coupling between MIMO elements.

As a start, two antennas were considered to study the mutual coupling between them, then reducing it by using some well-known techniques and transferring those techniques to the suggested models consisting of four antennas. Figure 7(a) shows the two separate ports antennas with a separation distance (S) between elements of half wavelength ($\lambda/2$). The mutual coupling at the frequency of 30 GHz is about -21.4 dB as shown in Figure 7(b). Three methods were used to reduce mutual coupling

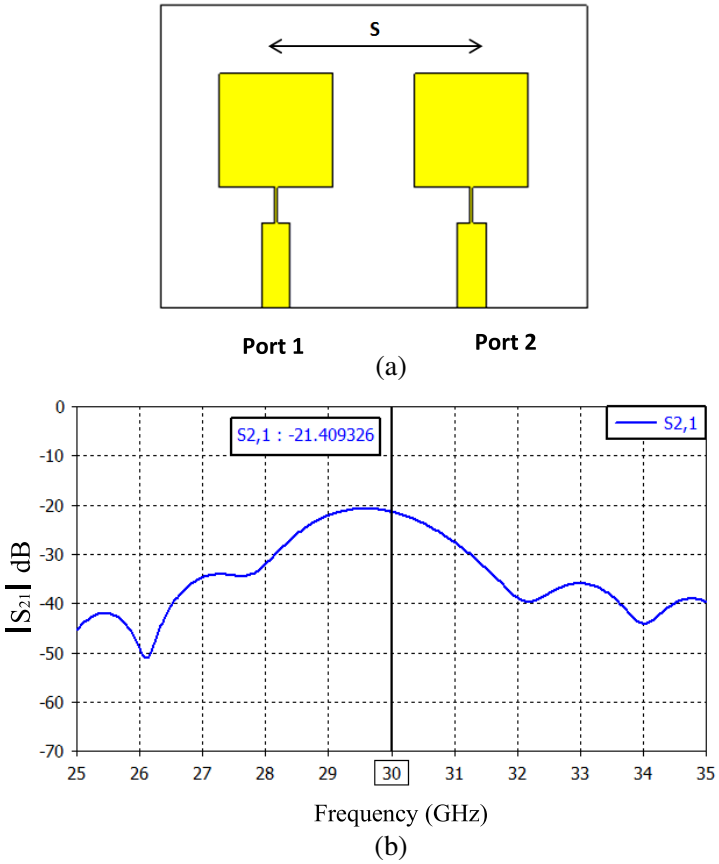

Figure 7. (a) Two microstrip patch antennas. (b) Mutual coupling between ports.

as much as possible which are Curved Edges CE, Defected Ground Structure (DGS), and Band Gap Structure (BGS).

In CE technique, cuts are made in the patch corners to be in a curved shape in order to reduce the mutual coupling between the elements. As shown in Figure 8(a) a cutting of quarter of a circle with a radius of 2 mm was made to form the curved edges. This cutting allows reducing the energy coming out of all the elements corners and reducing the flow to the neighboring elements and accordingly reduces the surface current propagation. Figure 8(b) shows the coupling coefficient after curving the corners which is reduced to −22.7 dB at 30 GHz.

In DGS, an intentional deformation is made on the ground plane to improve overall performance. The symmetric DGS added below the substrate acts as a resonant gap, and the current distribution in the ground plane varies depending on the size and shape of the deformation. These deformations control the electromagnetic propagation and excitation that passes through the substrate. Sometimes DGS results in multiple frequencies, making the antenna operate on more than one frequency (multiband) or operates on a wide band. As shown in Figure 9(a), the DGS is a ring with a radius of 0.7 mm and a width of 0.2 mm. The separation distance between rings was optimized by Particle Swam Optimizer of the CST, and it was found that the best isolation values appear with the values shown in Table 1.

Table 1. Detailed dimensional parameters (mm).

Symbols	Lp	Li	Lm	S	r	C	Lb	Mb	Wb
Dimensions (mm)	3.160	1.000	2.405	5.000	5.200	7.300	0.689	0.026	0.053

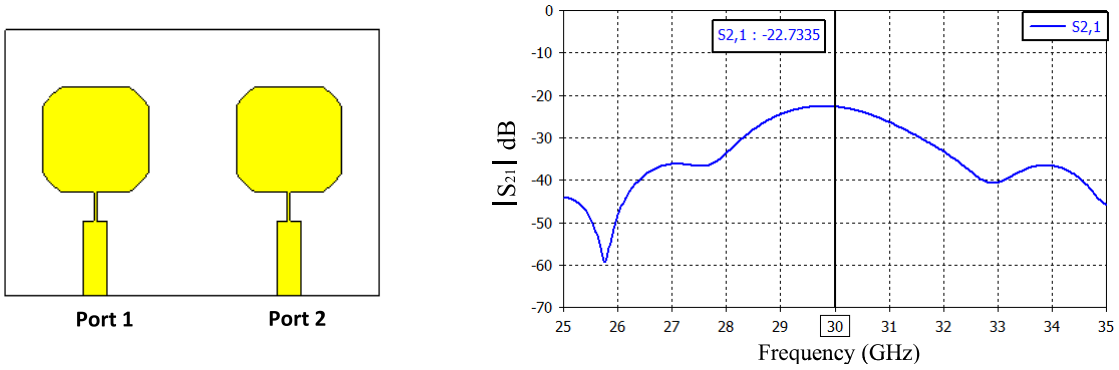

(a) (b)

Figure 8. (a) Shape of antenna after making curved edges. (b) Mutual coupling after making curved edges.

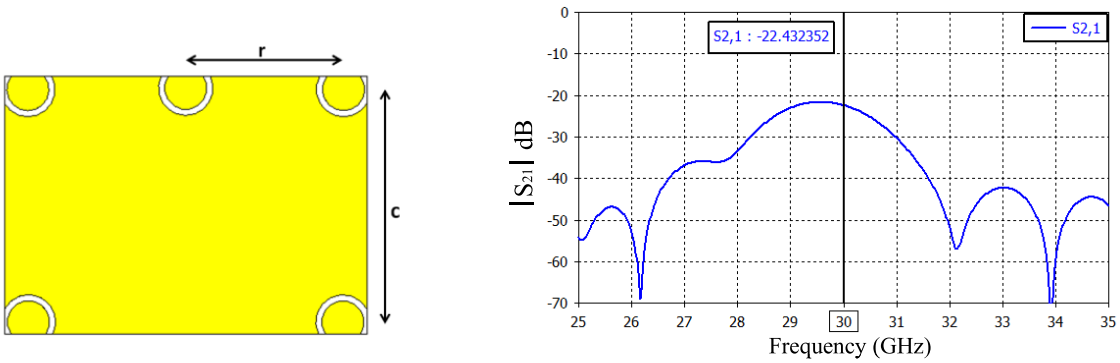

(a) (b)

Figure 9. (a) Shape of ground plane after making DGS. (b) Mutual coupling after making DGS.

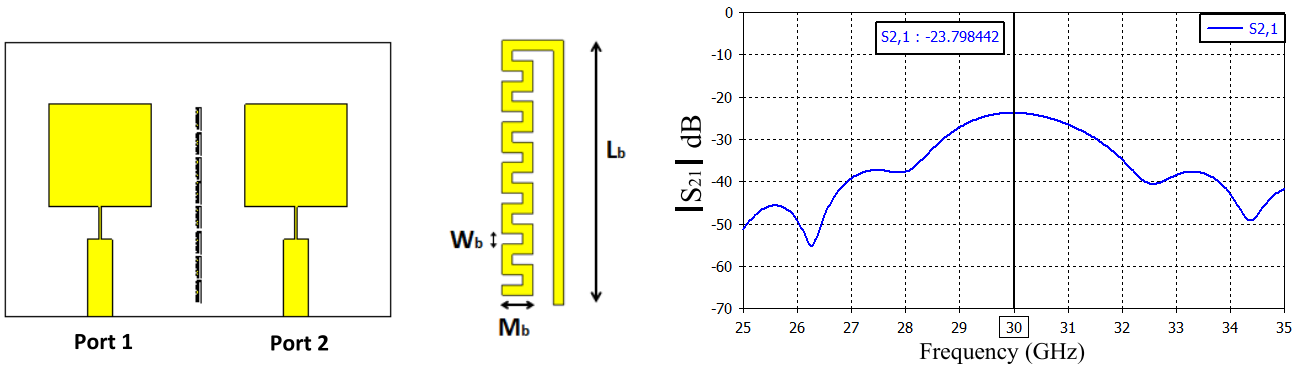

(a) (b) (c)

Figure 10. (a) Shape of antenna after adding BGS. (b) Shape of BGS. (c) Mutual coupling after adding BGS.

Electromagnetic Band-Gap or known as Band-Gap Structure (BGS) is one of the best methods used to reduce mutual coupling between ports and elements. The BGS technique has two main advantages. The first is to prevent surface waves from propagating at certain frequencies, and the second is the ability to make the incident waves reflect in phase rather than reflect out of phase, so the antenna can be attached very closely to the BGS, which helps to reduce the overall size of the MIMO antenna. Figures 10(a) and (b) show the shape and location of the BGS. The dimensions of the BGS were

optimized by Particle Swam Optimizer of the CST. Table 1 shows the optimized dimensions for the best isolation.

All the improvements were studied separately, and then all the modifications were assembled together. It was found that the mutual coupling is equal to −21.3 dB without any modification. Figure 8(b) shows the improvement to −22.7 dB when curved edges were made.

Figure 9(b) shows that the mutual coupling value became −22.4 dB when the Defected Ground Structure (DGS) was only added on the ground plane. Mutual coupling is found to be −23.7 dB when the band gap structure (BGS) was added as shown in Figure 10(c).

The final shape of the antenna after adding all the techniques used to reduce mutual coupling is shown in Figure 11(a). It turns out that the mutual coupling became −27.2 dB at a frequency of 30 GHz which means reduction by about 6 dB as shown in Figure 11(b). Table 2 summarizes the modifications created using each method. Figure 12 shows the clear moving surface current between two antenna elements. Figure 13 shows the surface current after adding CE, DGS, and BGS, and it is clear that the current decreased between the two elements. Figure 14 shows the comparison in the values of the mutual coupling between elements without modifications and after adding all of them.

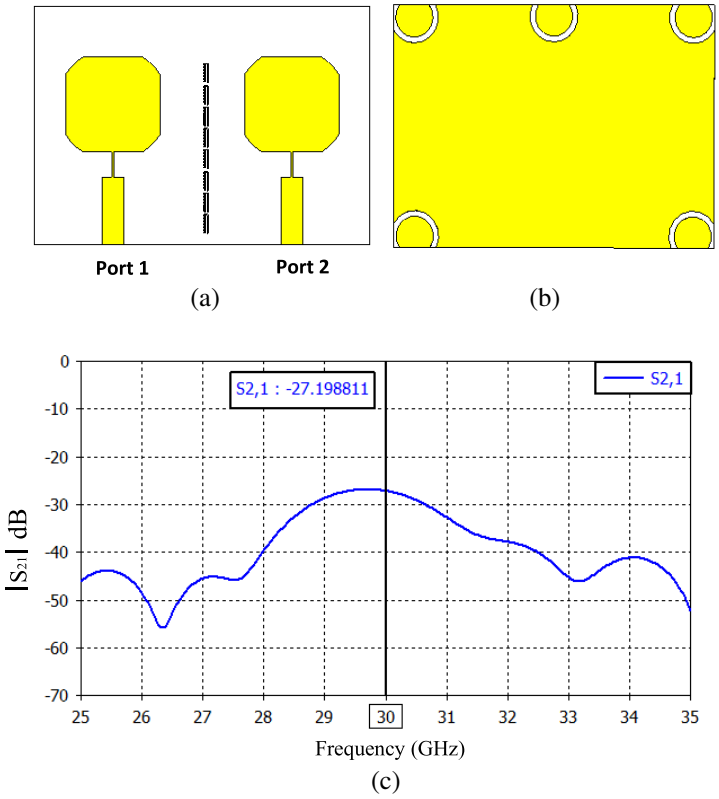

Figure 11. Shape of antenna after adding all modifications, (a) front side, (b) backside and (c) mutual coupling after adding all modifications.

4. DESIGN OF FOUR ELEMENTS MIMO ANTENNA

MIMO antenna system was designed using four elements as shown in Figure 15. All the techniques that were used in the case of two elements were added as shown in Figure 16. Photos of the fabricated four MIMO antennas configuration with all modifications are shown in Figure 17. It is clear that there is a good improvement in the mutual coupling between the ports. For example, when taking port No. 2 and studying the effect of the surrounding ports on it, we can find that there is improvement in S-parameters in both simulations and measurements as shown in Figure 18. S_{12} improved from −22.6 dB

Table 2. Results of modifications (dB).

Type of antenna	S_{21} (at 30 GHz)
Two antennas	−21.4
Two antennas with curved edges	−22.7
Two antennas with DGS	−22.4
Two antennas with BGS	−23.7
Two antennas with curved edges, BGS and DGS	−27.2

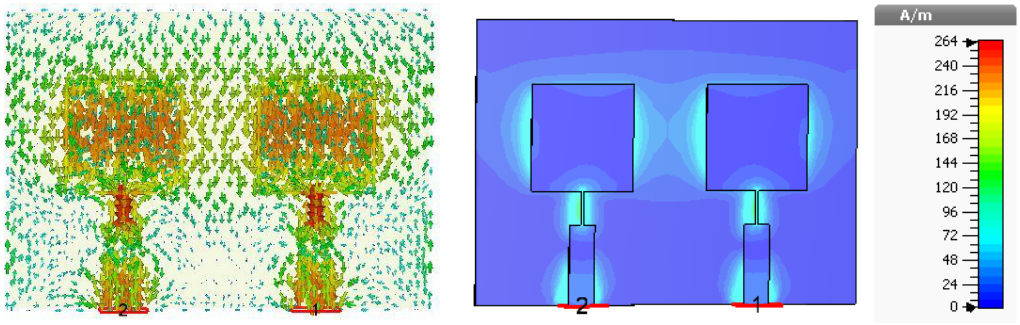

Figure 12. Surface current without modification.

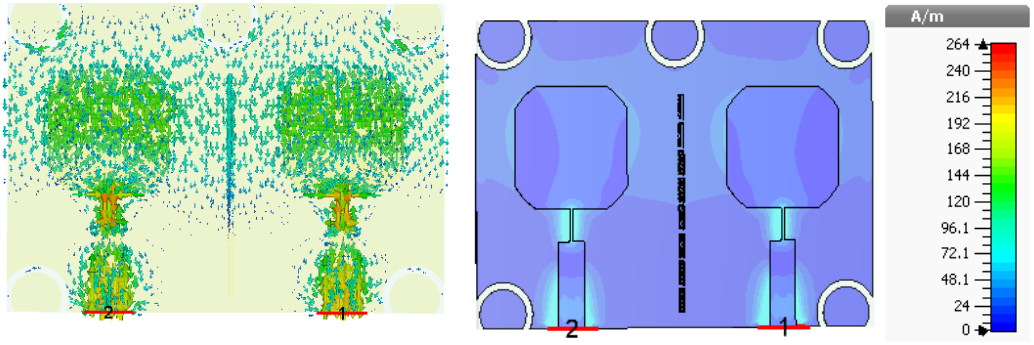

Figure 13. Surface current with all modification.

to −27.6 dB; S_{32} improved from −23.1 to −27.8 dB; and S_{42} improved from −32.8 to −37.4 dB. The Envelope Correlation Coefficient (ECC) is used to determine the correlation between the radiation patterns of two antennas. For example, the value of ECC is nearly zero when the polarization of one antenna is vertical, and the other is horizontal. The value of ECC is 1 when the polarizations of the two antennas are in the same direction. The value of the ECC can be calculated in two ways. The first is by using Eq. (1) where F is the radiation pattern, and the second is by using the S-parameters as shown in Eq. (2). Accordingly, the diversity gain (DG) can be calculated as shown in Eq. (3) [25].

$$\mathrm{ECC} = \frac{\left|\iint \overline{F_1} \cdot \overline{F_2^*} d\Omega\right|^2}{\iint \left|\overline{F_1}\right|^2 d\Omega \cdot \iint \left|\overline{F_2}\right|^2 d\Omega} \tag{1}$$

$$\mathrm{ECC} = \frac{\left|S_{11}^* S_{12} + S_{21}^* S_{22}\right|^2}{\left(1 - \left|S_{11}\right|^2 - \left|S_{21}\right|^2\right)\left(1 - \left|S_{22}\right|^2 - \left|S_{12}\right|^2\right)} \tag{2}$$

$$\mathrm{DG} = 10\sqrt{1 - (\mathrm{ECC})^2} \tag{3}$$

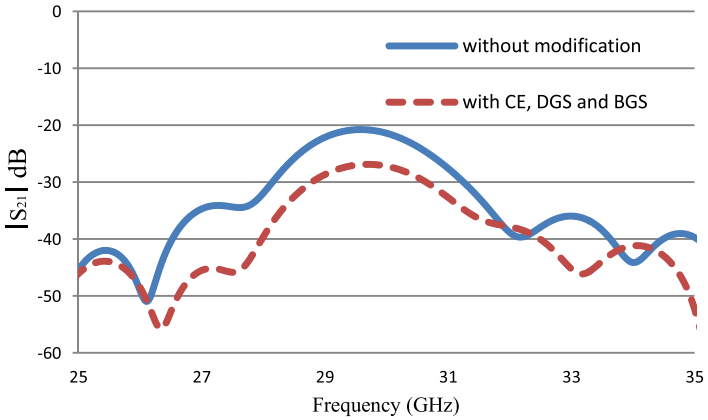

Figure 14. S_{21} results after and before modifications.

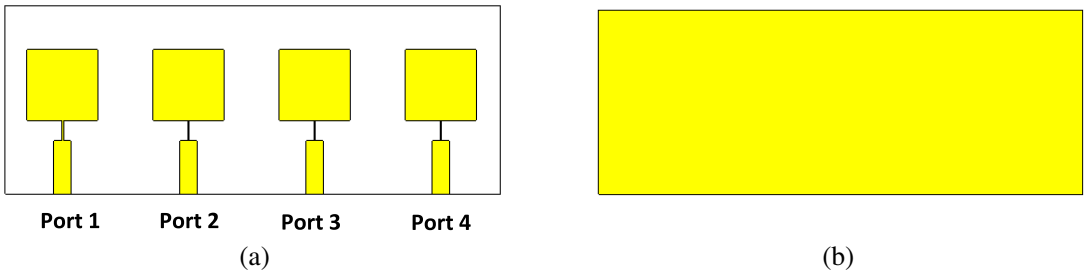

Figure 15. Four MIMO antenna configuration without modifications. (a) Front side and (a) backside.

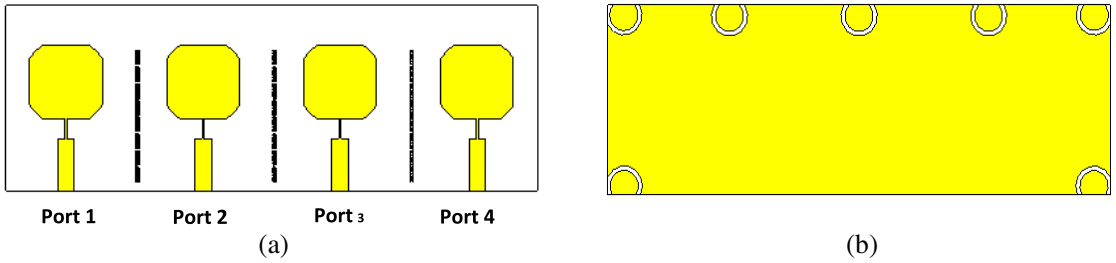

Figure 16. Four MIMO antenna configurations with all modifications. (a) Front side and (a) backside.

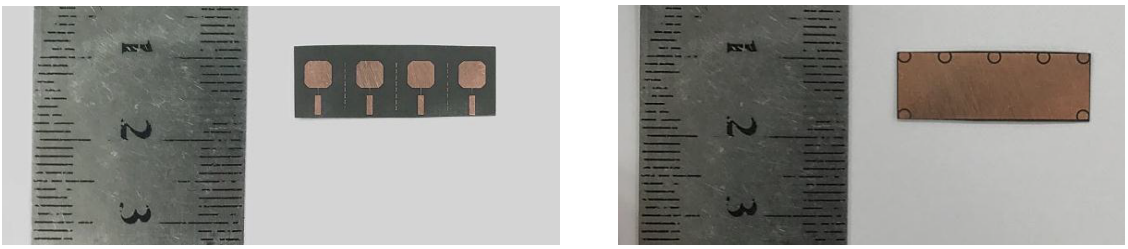

Figure 17. Photo of the fabricated four MIMO antenna configuration with all modifications. (a) Front side and (a) backside.

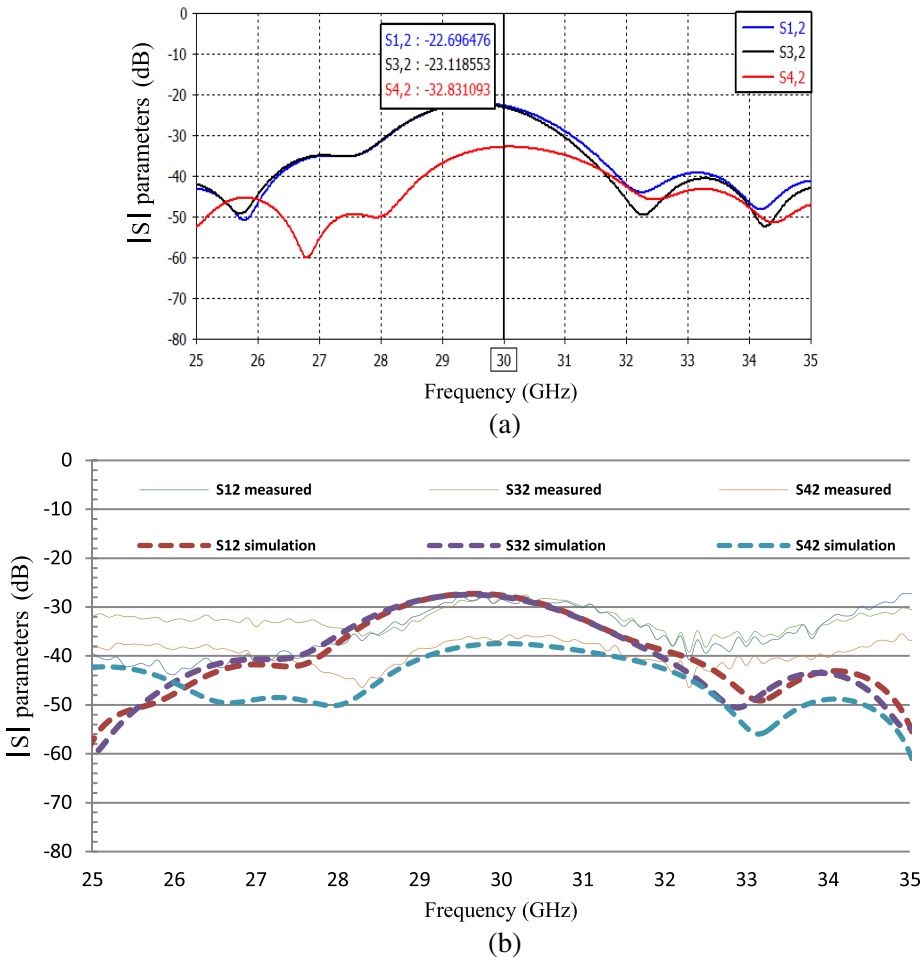

Figure 18. (a) S-parameters of port No. 2 without any modifications. (b) S-parameters of port No. 2 with all modifications.

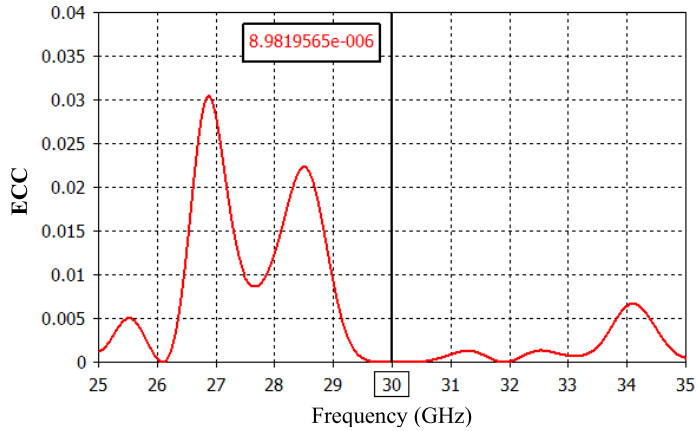

Figure 19. Envelope correlation coefficient of MIMO antenna configuration between port 1 and port 2.

Figure 19 shows the value of the envelop correlation coefficient between port 1 and port 2. It is clear that its value is close to zero. Figure 20 shows the diversity gain of the MIMO antenna. The radiation efficiency of this MIMO antenna is nearly 85% as shown in Figure 21.

Another MIMO antenna configuration was designed using four elements placed sequential to each

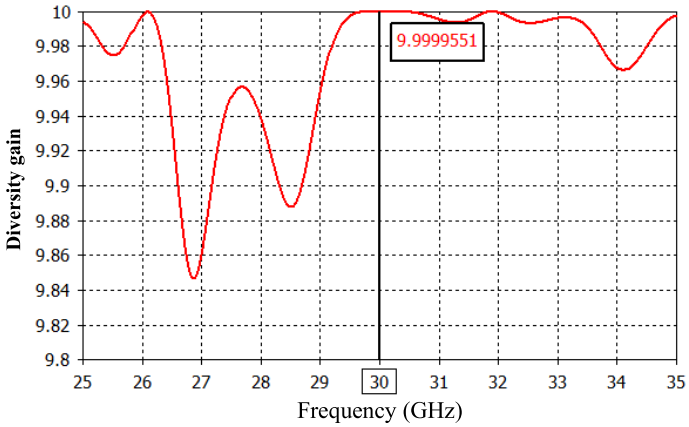

Figure 20. Diversity gain of MIMO antenna configuration.

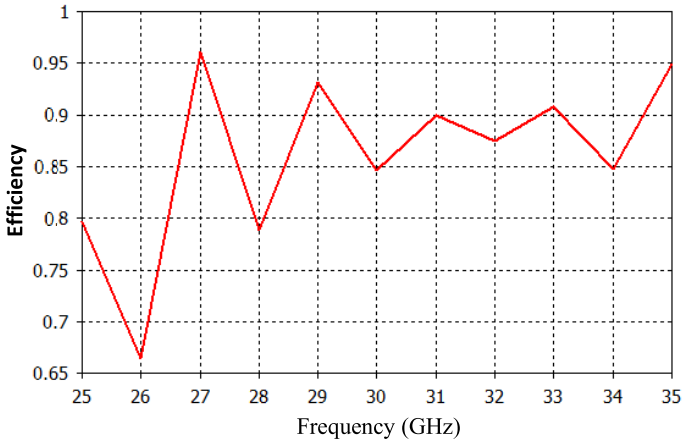

Figure 21. Efficiency across frequency.

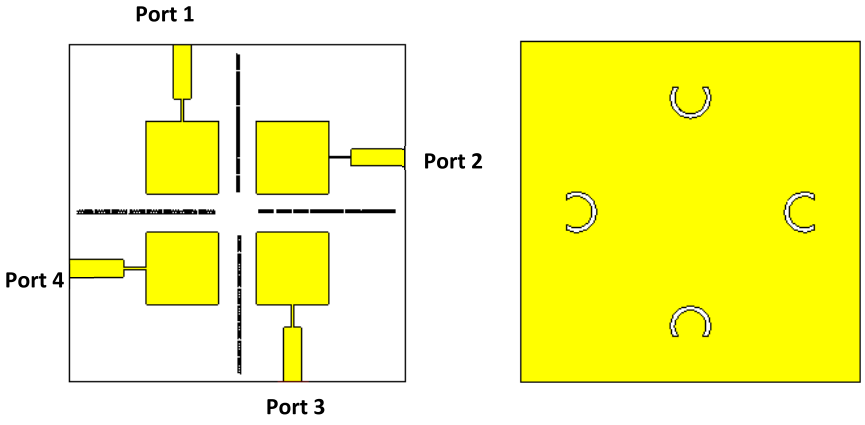

Figure 22. Four sequential MIMO antennas with all modifications. (a) Front side and (a) backside.

other adding DGS and BGS that were used on the two elements configuration as shown in Figure 22. Photos of the fabricated four MIMO antennas with all modifications are shown in Figure 23.

Figure 24 shows an improvement in S-parameters. S_{12} improved from -39.5 dB to -41.8 dB; S_{32} improved from -48.9 to -55.3 dB; and S_{42} improved from -42 to -48 dB. Figure 25 shows the value

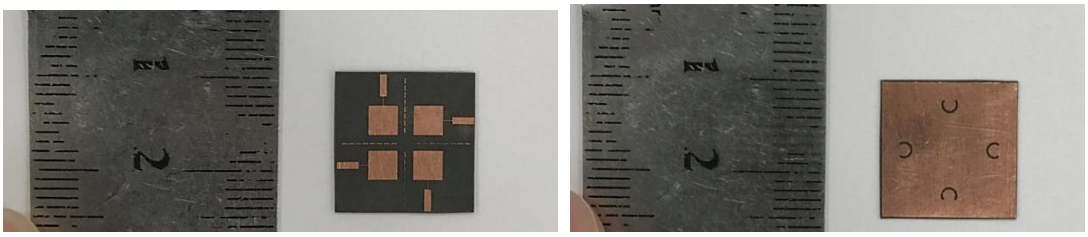

(a) (b)

Figure 23. A photo of the fabricated sequential four element MIMO antenna with all modifications. (a) Front side and (a) backside.

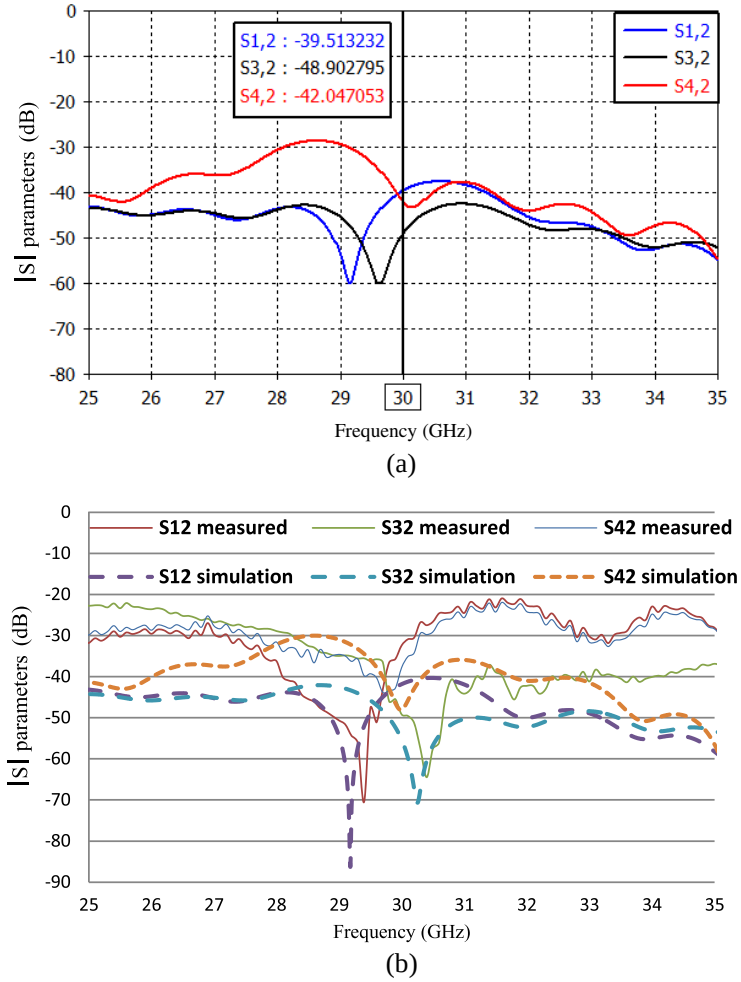

Figure 24. (a) S-parameters of port No. 2 without any modifications. (b) S-parameters of port No. 2 with all modifications.

of the envelop correlation coefficient between port 1 and port 2 at 30 GHz which is about 1.9×10^{-6}. Figure 26 shows the diversity gain of the MIMO antenna which reaches a value of about 9.99. Also, the radiation efficiency is about 83% as shown in Figure 27. The radiation efficiency is slightly reduced as a side effect of mutual coupling reduction, knowing that it was 87.5% before modifications. Accordingly, this MIMO sequential antenna configuration shows good performance suitable for operation in the fifth-generation applications and can work in almost all smart devices.

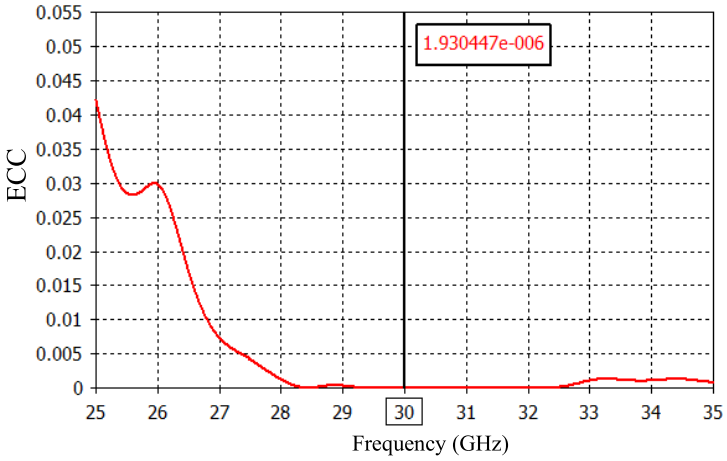

Figure 25. Envelope correlation coefficient of MIMO antenna.

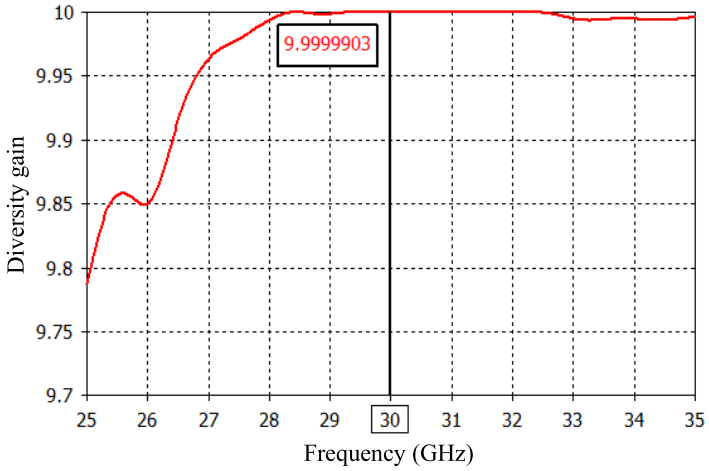

Figure 26. Diversity gain against frequency.

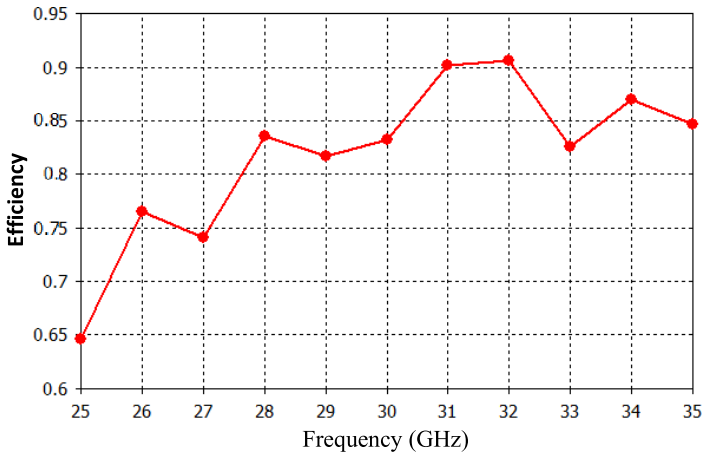

Figure 27. Radiation efficiency across frequency.

5. CONCLUSION

The core of this paper is to reduce the mutual coupling reduction in the proposed MIMO antennas configurations. Curved Edges (CE), Defected Ground Structure (DGS), and Band Gap Structure (BGS) were the mutual coupling reduction techniques used. Two MIMO antenna configurations that could serve 5G applications were introduced. The first MIMO antenna configuration consists of four linear rectangular elements connected to an impedance transformer to reduce mutual coupling. S_{12}, S_{32}, and S_{42} show improvement from -22.6 dB to -27.6 dB, from -23.1 to -27.8 dB, and from -32.8 to -37.4 dB, respectively. The second MIMO antenna configuration consists of four antennas arranged sequentially. The scattering parameters S_{12}, S_{32}, and S_{42} were improved from -39.5 dB to -41.8 dB, from -48.9 to -55.3 dB, and from -42 to -48 dB, respectively. From the simulated far field radiation patterns using Computer Simulation Technology (CST) and High Frequency Structure Simulation Software (HFSS), directivity is equal to 8.2 dBi, and the gain is around 7.5 dBi at 30 GHz. ECC value was close to zero. The MIMO antenna's diversity gain is close to ten, and its radiation efficiency is close to 85%. To verify our results, prototypes of the designed MIMO configurations have been fabricated. Measurements of the fabricated prototypes show agreement with simulation results.

REFERENCES

1. Rappaport, T. S., S. Sun, R. Mayzus, et al., "Millimeter wave mobile communications for 5G cellular: It will work!" *IEEE Access*, Vol. 1, 335–349, 2013.
2. Pi, Z. and F. Khan, "An introduction to millimeter-wave mobile broadband systems," *IEEE Communications Magazine*, Vol. 49, No. 6, 101–107, Jun. 2011.
3. Rappaport, T. S., J. N. Murdock, and F. Gutierrez, "State of the art in 60-GHz integrated circuits and systems for wireless communications," *Proceedings of the IEEE*, Vol. 99, No. 8, 1390–1436, Aug. 2011.
4. Wang, C.-X., F. Haider, X. Gao, et al., "Cellular architecture and key technologies for 5G wireless communication networks," *IEEE Communications Magazine*, Vol. 52, No. 2, 122–130, Feb. 2014.
5. Wei, L., R. Q. Hu, Y. Qian, and G. Wu, "Key elements to enable millimeter wave communications for 5G wireless systems," *IEEE Wireless Communications*, Vol. 21, No. 6, 136–143, Dec. 2014.
6. Li, Q., G. Li, W. Lee, et al., "MIMO techniques in WiMAX and LTE: A feature overview," *IEEE Communications Magazine*, Vol. 48, No. 5, 86–92, May 2010.
7. Qualcomm Technologies Inc., "Spectrum for 4G and 5G," Qualcomm Technologies Inc., Dec. 2017, [online]. Available: https://www.qualcomm.com/news/media-center. [Accessed Jan. 5, 2019].
8. Liu, D., W. Hong, T. S. Rappaport, et al., "What will 5G antennas and propagation be?" *IEEE Trans. Antennas Propag.*, Vol. 65, No. 12, 6205–6212, 2017.
9. Rappaport, T. S., Y. Xing, G. R. MacCartney, et al., "Overview of millimeter wave communications for fifth-generation (5G) wireless networks — With a focus on propagation models," *IEEE Trans. Antennas Propag.*, Vol. 65, No. 12, 6213–6230, 2017.
10. Yang, S. and L. Hanzo, "Fifty years of MIMO detection: The road to large-scale MIMOs," *IEEE Communications Surveys & Tutorials*, Vol. 17, No. 4, 1941–1988, 2015.
11. Hussain, R., A. T. Alreshaid, S. K. Podilchak, and M. S. Sharawi, "Compact 4G MIMO antenna integrated with a 5G array for current and future mobile handsets," *IET Microwaves Antennas and Propagation*, Vol. 11, No. 2, 271–279, 2017.
12. Li, Y., C. Wang, H. Yuan, N. Liu, H. Zhao, and X. Li, "A 5G MIMO antenna manufactured by 3-D printing method," *IEEE Antennas and Wireless Propagation Letters*, Vol. 16, 657–660, 2017.
13. Li, W.-A., Z.-H. Tu, and Q.-X. Chu, "Design of planar wideband MIMO antenna for mobile phones," *2015 IEEE International Wireless Symposium (IWS 2015)*, 1–4, Shenzhen, China, 2015.
14. Jilani, S. F. and A. Alomainy, "Millimetre-wave T-shaped antenna with defected ground structures for 5G wireless networks," *2016 Loughborough Antennas & Propagation Conference (LAPC)*, 1–3, Loughborough, UK, 2016.

15. Ou Yang, J., F. Yang, and Z. M. Wang, "Reducing mutual coupling of closely spaced microstrip MIMO antennas for WLAN application," *IEEE Antennas and Wireless Propagation Letters*, Vol. 10, 310–313, 2011.
16. Chiu, C.-Y., C.-H. Cheng, R. D. Murch, and C. R. Rowell, "Reduction of mutual coupling between closely-packed antenna elements," *IEEE Trans. Antennas Propag.*, Vol. 55, No. 6, 1732–1738, Jun. 2007.
17. Hammoodi, A. I., A. Isaac, H. Raad, and M. Milanova, "Mutual coupling reduction between two closely spaced PIFAs," *2018 IEEE International Symposium on Antennas and Propagation & USNC/URSI National Radio Science Meeting*, 1367–1368, Boston, MA, USA, 2018.
18. Lotfi Neyestanak, A. A., F. Jolani, and M. Dadgarpour, "Mutual coupling reduction between two microstrip patch antennas," *2008 Canadian Conference on Electrical and Computer Engineering*, 739–742, Niagara Falls, ON, Canada, 2008.
19. Rusek, F., D. Persson, B. K. Lau, et al., "Scaling up MIMO: Opportunities and challenges with very large arrays," *IEEE Signal Processing Magazine*, Vol. 30, No. 1, 40–60, Jan. 2013.
20. Nadeem, I. and D.-Y. Choi, "Study on mutual coupling reduction technique for MIMO antennas," *IEEE Access*, Vol. 7, 563–586, 2019, doi: 10.1109/ACCESS.2018.2885558.
21. Khandelwal, M. K., B. K. Kanaujia, and S. Kumar, "Defected ground structure: Fundamentals, analysis, and applications in modern wireless trends," *International Journal of Antennas and Propagation*, Vol. 2017, 22 pages, Article ID 2018527, 2017.
22. Yang, F. and Y. Rahmat-Samii, "Applications of electromagnetic band-gap (EBG) structures in microwave antenna designs," *2002 3rd International Conference on Microwave and Millimeter Wave Technology, 2002. Proceedings. ICMMT 2002*, 528–531, Beijing, China, 2002.
23. Cheng, B. and Z. Du, "Dual polarization MIMO antenna for 5G mobile phone applications," *IEEE Trans. Antennas Propag.*, Vol. 69, No. 7, 4160–4165, Jul. 2021.
24. Allah, A., H. Ahmad, M. Sohail, W. Zaman, M. Ismail, and M. Rahman, "A novel high gain array approach MIMO antenna operating at 28 GHz for 5G mmWave applications," *2021 1st International Conference on Microwave, Antennas & Circuits (ICMAC)*, 1–4, 2021.
25. Vaughan, R. G. and J. B. Andersen, "Antenna diversity in mobile communications," *IEEE Transactions on Vehicular Technology*, Vol. 36, No. 4, 149–172, Nov. 1987.